Response to Referee #1

General comments:

This manuscript integrates multi-source InSAR observations with hydrological recession analysis to investigate permafrost-related surface deformation and its hydrological implications in a disturbed alpine river basin. The study addresses an important topic in cryosphere–hydrology interactions, and the development of a long-term deformation dataset is a valuable contribution to the community. The joint analysis of InSAR deformation and hydrology recession analysis is novel, and overall it is well done. I have some concerns on the methodology development and analysis that need to be clarified or discussed before the publication. Details are provided as below.

Response: We thank the reviewer for the positive assessment and constructive comments. In response, we have: (1) discussed the limitations of the linear–periodic temporal constraint and the ALOS-2 derived velocity reference, and evaluated interannual Sentinel-1 interferograms and compared their performance with that of the ALOS-2 constrained NSBAS approach; (2) quantified the interannual stability of the thaw-season deformation scaling factors; (3) examined the temporal variability of the recession parameter b; and (4) applied Geodetector factor analysis to rank the explanatory power of environmental controls on seasonal deformation spatial variability. The relevant methods, results, discussion, figures, and supplementary materials have been revised accordingly. Detailed responses are provided below:

1. InSAR processing

The deformation analysis relies primarily on descending-orbit SAR acquisitions. While limited data availability may justify this choice for earlier sensors, Sentinel-1 provides systematic coverage in both ascending and descending tracks over most land areas. The authors should clarify the rationale for restricting the Sentinel-1 analysis to descending data.

Response: Thank you for the comment. For Sentinel-1, the descending track was selected mainly because it offers more frequent acquisitions and better temporal continuity over the study area. The ascending track contains several longer temporal gaps that would reduce the connectivity of the interferogram network and potentially introduce greater uncertainty into the time-series inversion, as shown in Fig. R1 (revised Fig. S2). We have briefly explained in Section 3.1.1 why we limit our work to descending tracks even though both ascending and descending tracks are available.

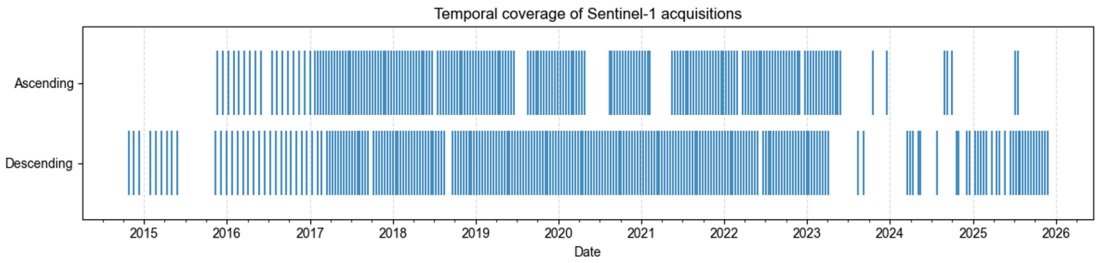

Fig. R1 (Revised Figure S2) Temporal distribution of ascending and descending Sentinel-1 acquisitions of the study area

Line 160-: *"For the later period, Sentinel-1 provides dense observations suitable for deformation time series inversion. Although both ascending and descending tracks are available over the study area, the descending track has more frequent acquisitions and shows better temporal continuity, whereas the ascending observations contain several extended temporal gaps (Fig. S2), which would reduce the stability of the time series inversion (Li et al., 2022b). The descending track was therefore selected to ensure better interferogram network connectivity."*

The SAR datasets used in this study also differ in temporal coverage and observation periods. The potential impact of these inconsistencies on the long-term deformation estimates, as well as the associated uncertainties, need to be more explicitly discussed.

Response: Thank you for this comment. As suggested, we have expanded the discussion in Section 5.2 to more explicitly address the impacts of differing temporal coverage and observation periods on the long-term deformation estimates.

Line 588-: *"While multi-source SAR data allow for long-term trend detection, the inherent differences in radar wavelengths (C-band vs. L-band), acquisition geometries (including incidence angles and orbital directions), temporal coverage and observation periods might introduce uncertainties into the derived long-term deformation trends to some extent."*

Line 628-: *"The ERS-2, Envisat, and ALOS-1/2 results were derived from sparse interferograms and therefore represent interval-averaged deformation rates. These observations remain suitable for identifying broad stage-scale deformation differences but provide less information on short-term or nonlinear variations and the precise identification of abrupt deformation changes. In addition, temporal gaps between SAR observation periods leave deformation during these intervals unobserved. The combined results are regarded as a sequence of period-specific estimates rather than a fully continuous deformation record referenced to a common epoch."*

The study addresses the poor quality of C-band interferograms during winter, likely caused by snow cover and freeze–thaw-related decorrelation, by applying a linear–periodic temporal constraint within the NSBAS-InSAR framework and by calibrating the Sentinel-1 time series using ALOS-2-derived deformation rates. The NSBAS time-series inversion is constrained using long-term deformation rates derived from ALOS-2 data. While this approach is practical, the imposed constraints and simplified temporal model may not fully capture complex or transient deformation signals. A discussion of the limitations of this methodology, and how they may influence the reconstructed long-term deformation time series, would help clarify the strength and advantages of the method. In addition, previous studies have attempted to mitigate winter decorrelation in C-band InSAR over permafrost regions by using long-temporal-baseline interferograms acquired during summer-to-summer periods, which can avoid snow-contaminated winter acquisitions and has been shown to perform well in Alaska (Guan, S.; Wang, C.; Tang, Y.; Zou, L.; Yu, P.; Li, T.; Zhang, H. (2024). North American Circum-Arctic Permafrost Degradation Observation Using Sentinel-1 InSAR Data. Remote Sensing, 16(15), 2809. DOI: 10.3390/rs16152809). It would be useful for the authors to discuss this alternative strategy and compare its advantages and limitations with the ALOS-2-constrained approach used in this study. Such a discussion would better clarify the methodological applicability, and potential limitations of the proposed approach.

Response: Thank you for the constructive comments. We agree that the imposed temporal model and the ALOS-2-derived velocity reference may affect the reconstructed Sentinel-1 deformation time series. We have expanded Section 5.2 to discuss these limitations.

Line 595-: *"……, we implemented a data-constrained NSBAS approach that incorporated ALOS-2 L-band deformation rates as reference information. This approach takes advantage of the high and spatially continuous coherence of the L-band observations to constrain the long-term deformation trend. Nevertheless, the ALOS-2 reference represents a long-term mean deformation rate, and the linear–periodic temporal constraint may not fully resolve interannual or transient deformation variability within the Sentinel-1 network gaps. The deformation rate derived from the sparse D-InSAR pairs may also be susceptible to local noise and atmospheric effects (Li et al., 2022). Moreover, ALOS-2 covers only part of the Sentinel-1 study area, the reference velocity outside the overlapping region was obtained by extending the CDF matching correction, which may not fully represent local deformation variability."*

Following the suggestion, we also examined interannual Sentinel-1 interferograms acquired near the end of thawing seasons and evaluated both their coherence and spatial deformation patterns (Figs. R2 & R3). While some interferograms retained moderate coherence (0.4-0.7) and spatially continuous deformation signals, fragmented low-coherence areas can introduce localized phase unwrapping errors as

shown in Fig. R3. In contrast, the ALOS-2 interannual interferograms maintained substantially higher and more spatially continuous coherence, providing more reliable deformation estimates. More details were provided in Section 5.2 as below:

Line 603-: *"An alternative strategy is to connect annual thaw-season networks using interannual Sentinel-1 interferograms acquired near the end of the thawing season (Guan et al., 2024). This approach avoids cross-frequency inconsistencies and requires no additional data. In our study area, these interferograms achieved moderate spatially averaged coherence (0.4–0.7, Fig. S15). Some interferograms, such as the 2019–2020 interferogram (Fig. S16), retained relatively high coherence and spatially continuous deformation signals, demonstrating the potential feasibility of this strategy. However, the coherence maps show strong heterogeneity within most interferograms, and fragmented low-coherence areas can reduce the spatial continuity of reliable phase retrieval and increase susceptibility to phase unwrapping errors (Oliver-Cabrera et al., 2022). For example, localized unwrapping errors were evident even in a relatively high coherence interferogram, appearing as abrupt deformation jumps relative to the surrounding deformation field, as shown in Fig. S16. In contrast, the ALOS-2 L-band interferograms maintained high and spatially continuous coherence (>0.95, Fig. S8) over long temporal baselines, providing a more stable and reliable reference for the long-term deformation trend."*

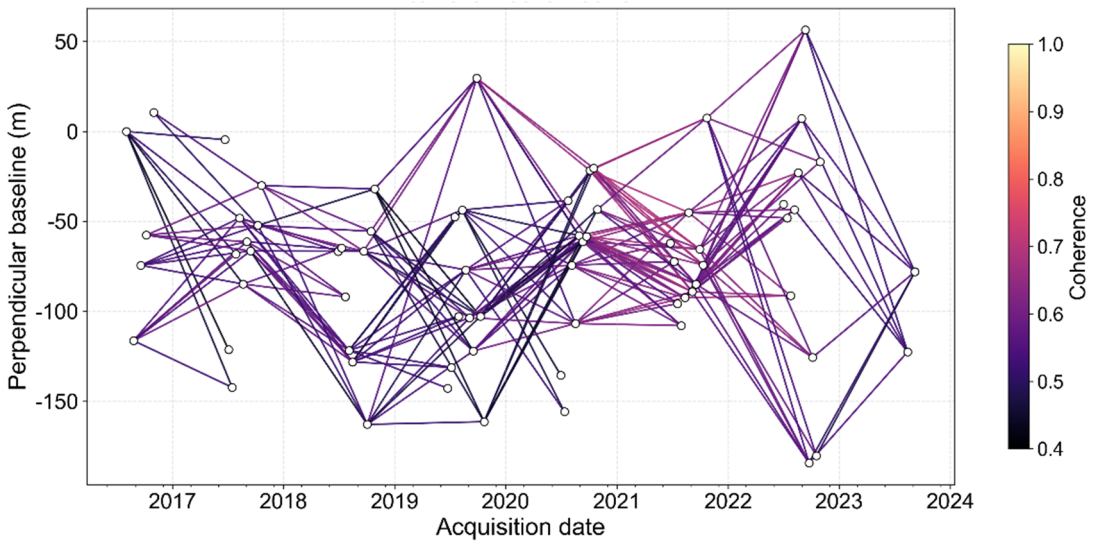

Fig. R2 (Revised Figure S15) The network of the interannual Sentinel-1 interferograms acquired near the end of the thawing season, colored using the spatial mean coherence.

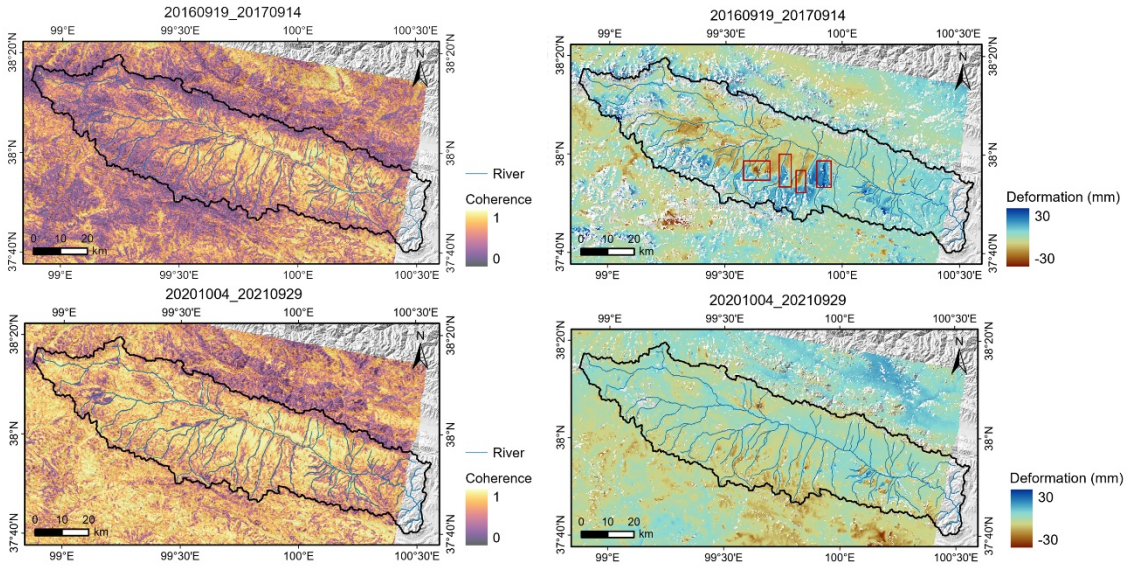

Fig. R3 (Revised Figure S16) Coherence and deformation maps of two representative interannual Sentinel-1 interferograms selected for their relatively high coherence. The red boxes indicate localized abrupt deformation discontinuities and sign reversals associated with likely phase unwrapping errors. The interferograms were generated using the Alaska Satellite Facility HyP3 processing service.

2. Uncertainty of the thaw-season deformation scaling

The thaw-season deformation scaling approach assumes that the relative proportions of deformation across different sub-periods remain stable across years. While practical, this assumption may be influenced by interannual variability in the climate conditions. Assessing the variability of the scaling factor across Sentinel-1 observational period, and providing an estimate of the associated uncertainty, would help evaluate the robustness of this approach.

Response: Thank you for the suggestion. To evaluate the potential uncertainty associated with the thaw-season deformation scaling approach, we calculated the standard deviation (STD) and coefficient of variation (CV) of the scaling factor for each of the four sub-periods, based on the Sentinel-1 deformation time series from 2016 to 2022. At the basin scale, the mean scaling factors range from 1.61 to 2.50, with STDs of 0.16–0.23 and CVs of 0.08–0.11 across four sub-periods. The results indicate that the scaling factors are generally stable across years, particularly within the main subsiding regions. We have added a supplementary figure (Fig. R4; with statistics summarized in Table S2) and also a brief discussion on the associated uncertainty of this approach.

Line 637-: *"We evaluated this assumption using the Sentinel-1 time series from 2016 to 2022 by calculating the standard deviation (STD) and coefficient of variation (CV, defined as the ratio of STD to the mean) of the scaling factor for each sub-period (Fig. S19, Table S2). Across the four sub-periods, the spatially averaged STD ranged from*

0.16 to 0.23, while the corresponding CV ranged from 0.08 to 0.11. These relatively low values support the overall validity and robustness of the scaling assumption, particularly within the main subsiding regions. Nevertheless, year-to-year differences in climatic conditions may still affect the relative contribution of deformation during different stages to some extent."

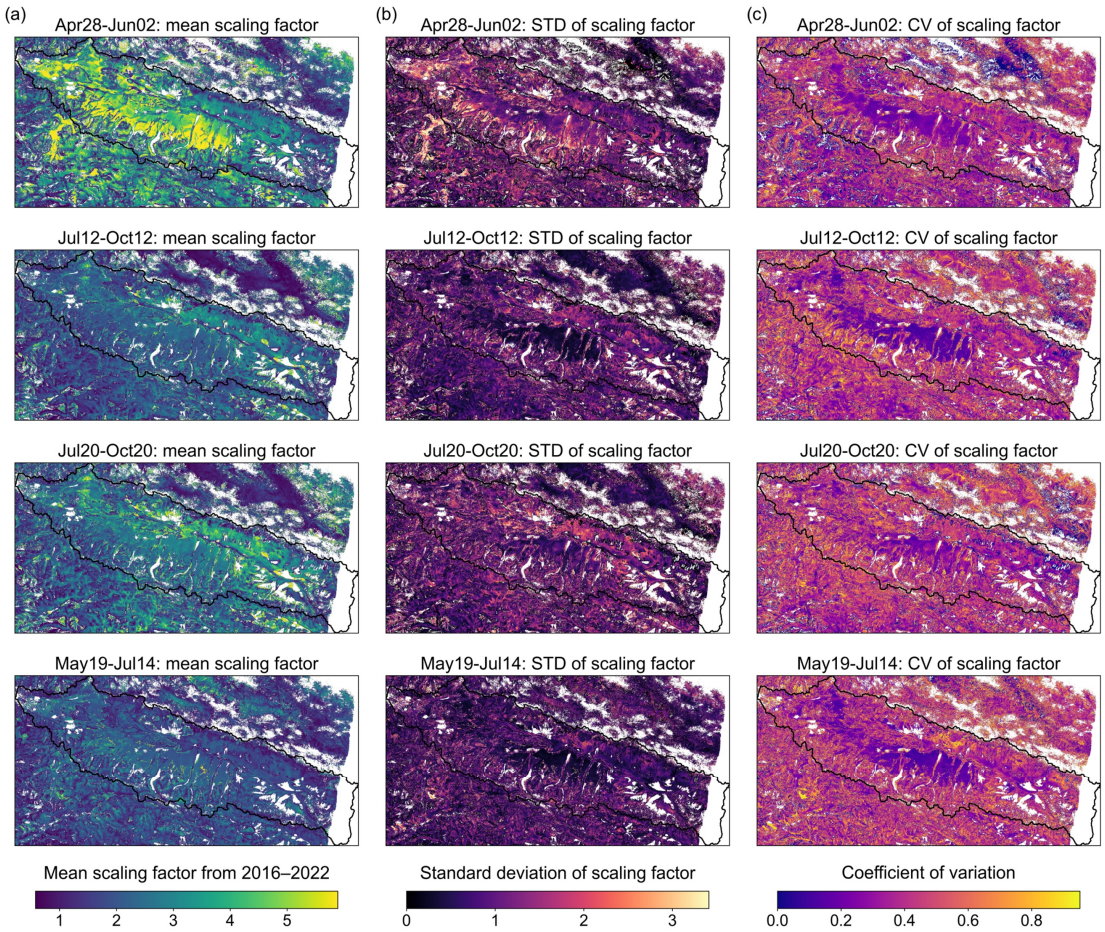

Fig. R4 (Revised Figure S19) Spatial variability and uncertainty of the thaw-season deformation scaling factors derived from the Sentinel-1 time series during 2016–2022. (a) temporal mean, (b) temporal standard deviation (STD), and (c) coefficient of variation (CV) for the four sub-periods.

Revised Table S2 Basin-scale statistics of the scaling factor from 2016 to 2022

Period	Mean	STD	CV	Min	Max
Apr28–Jun02	2.50	0.19	0.08	2.31	2.79
Jul12–Oct12	1.82	0.20	0.11	1.57	2.05
Jul20–Oct20	2.04	0.23	0.11	1.70	2.39
May19–Jul14	1.61	0.16	0.10	1.34	1.78

3. Recession analysis

The streamflow recession analysis provides some interesting insights. It is based on the power-law recession curve (Eq. 5), while the analysis focuses primarily on the recession rate (a). The other recession parameter (i.e. b) is also a key parameter controlling the nonlinearity of catchment drainage process. The authors may consider examining b, assessing its variability, and discussing its potential implications alongside with changes in a.

Response: Thank you for this valuable suggestion. We have examined the temporal variations in b, as shown in Fig. R5 (revised Fig. S13). The fitted b exhibited an overall increasing trend, with the most pronounced increase during the intensified period, indicating increasingly nonlinear recession behavior. This enhanced nonlinearity may reflect increased hydraulic connectivity and greater heterogeneity of subsurface drainage pathways following permafrost thaw (Hinzman et al., 2022). We have updated the results in Section 4.2 and discussed their potential implications in Section 5.1.

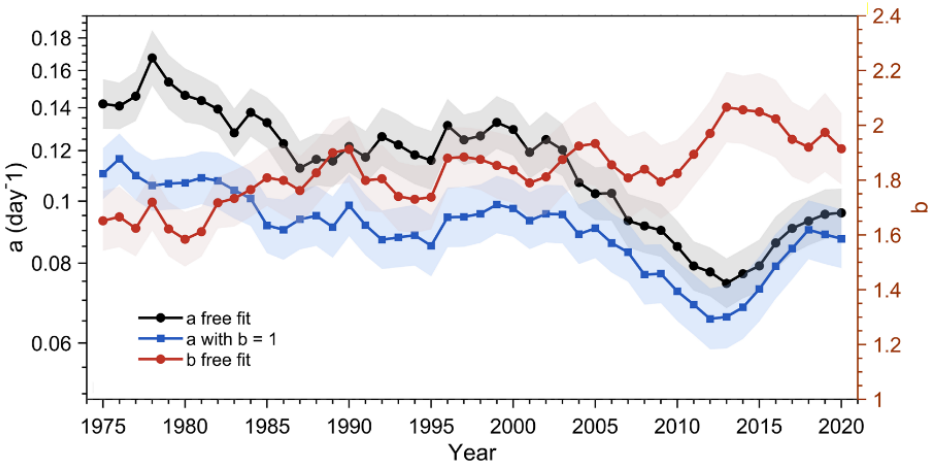

Fig. R5 (Revised Figure S13) Time series of recession rate (a) fitted from the free-b recession model, a fitted from the constrained model with b fixed to 1, and the time series of recession parameter b. Shaded areas indicate the 95% confidence intervals.

Line 300-: "b (dimensionless) is the recession shape index that reflects the shape and nonlinearity of the recession curve."

Line 322-: *"…… the parameter b was also obtained from each regression window to examine its temporal variability and assess its potential impacts on Ks."*

Line 478-: *"The parameter b exhibited an overall increasing trend from 1975 to 2020, with the most pronounced increase occurring during 2009–2013 (Fig. S13), coinciding with the period of intensified mining disturbance. This suggests that the recession process likely became more nonlinear (Hinzman et al., 2022)."*

Line 553-: *"The increase in b during the mining period indicates that the recession process became more nonlinear, further supporting a change in subsurface flow pathways. Permafrost thaw-induced increases in subsurface hydraulic connectivity and drainage heterogeneity may alter the contribution of supra- and sub-permafrost groundwater to baseflow (Hinzman et al., 2022). The interaction of these flow components with different drainage timescales results in a more nonlinear storage–discharge relationship."*

Reference:

Hinzman, A. M., Sjöberg, Y., Lyon, S., Schaap, P., & van der Velde, Y. (2022). Using a mechanistic model to explain the rising non-linearity in storage discharge relationships as the extent of permafrost decreases in Arctic catchments. Journal of Hydrology, 612, 128162. https://doi.org/10.1016/j.jhydrol.2022.128162

4. Quantitative attribution of environmental controls on deformation variability

The manuscript includes several environmental variables to interpret deformation patterns; however, their relative contributions are not well quantitatively assessed. It would be helpful if the authors could further clarify the relative importance of these factors, for example, by providing a ranking of explanatory power or applying a feature importance analysis.

Response: We appreciate this constructive suggestion. To better quantify the relative contributions of the environmental factors to the spatial variability of seasonal surface deformation, we applied the Geodetector method (Wang et al., 2016) and computed the q-statistic for each factor, which measures its explanatory power for the spatial variability of deformation. The new results were presented in Fig. R6 (Revised Figure 12). The results provide a clear ranking of explanatory power: ground ice content showed the highest q value ($q = 0.44$), followed by SWIR albedo ($q = 0.42$), slope ($q = 0.40$), NDVI (q=0.26), and thawing index ($q = 0.13$). Thus, ground ice content and SWIR albedo exerted strong controls on the spatial heterogeneity of seasonal deformation. The corresponding method and results have also been added to Sections 3.1.3 and 4.1.3, respectively.

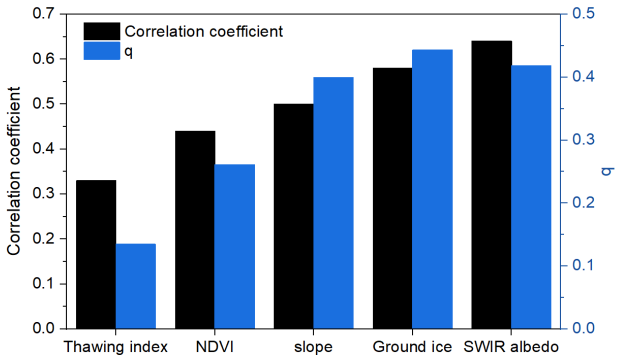

Fig. R6 (Revised Figure 12) The absolute correlation coefficients and Geodetector statistic q value of different environmental factors with deformation.

Line 256-: *"To explore the environmental controls on the spatial variability of surface deformation, correlation analyses and Geodetector factor analysis (Wang et al., 2016) were performed between InSAR-derived mean seasonal deformation and selected environmental factors……"*

Line 259-: *"Geodetector is a spatially stratified heterogeneity analysis method to detect associations between a spatial response variable and potential driving factors, and the Geodetector statistic* q *was used to evaluate the explanatory power of each factor for the spatial heterogeneity of seasonal deformation. The* q *statistic ranges from 0 to 1, with higher values indicating stronger explanatory power, and is defined as (Wang et al., 2016):*

$$q(Y|X) = 1 - \frac{-\sum_{h=1}^{L} N_h \sigma_h^2}{N\sigma^2}, \qquad (5)$$

where Y *denotes the seasonal deformation,* X *represents an environmental factor and* $h = 1, \ldots, L$ *denotes the strata or classes of the variable* Y *or influencing factor* X. N_h *and* σ_h^2 *are the number of spatial units and the variance of* σ_h^2 *within stratum* h*, respectively, whereas* N *and* σ^2 *are the total number of spatial units and the variance of* Y *over the entire study area."*

Lin 443-: *"Consistent with these correlation results, the Geodetector analysis identifies ground ice content (*$q = 0.44$*) and SWIR albedo (*$q = 0.42$*) as the dominant factors explaining the spatial variability of seasonal deformation, followed by slope (*$q = 0.40$*), whereas NDVI (*$q = 0.26$*) and thawing index (*$q = 0.13$*) exhibit comparatively weaker explanatory power."*

Reference:

Wang, J., Zhang, T., & Fu, B. (2016). A measure of spatial stratified heterogeneity. Ecological Indicators, 67, 250–256. https://doi.org/10.1016/j.ecolind.2016.02.052

Specific comments:

1. Section 3.1.1: It is unclear whether a consistent reference point is used across different InSAR data processing, which may affect the comparability of deformation estimates.

Response: Thank you for this comment. We have clarified the use and selection of the common reference point in Section 3.1.1:

Line 194-: *"A common reference point (38.0895°N, 99.7243°E) was used for all InSAR datasets to ensure the comparability of deformation estimates derived from different SAR sensors. The reference point was identified from Google Earth imagery as an exposed-bedrock surface outside the main deformation areas and exhibited high*

coherence (>0.95) and low temporal phase variability across the observation periods."

2. Line 255: Please clarify the temporal coverage of the datasets used in this analysis.

Response: Thank you for pointing this out. We have clarified the temporal coverage of all datasets used in the environmental-factor analysis.

Line 273-: *"While slope and ground ice content were treated as relatively static factors, NDVI, SWIR albedo, and the thawing index were derived as multi-year averages over 2016–2022, consistent with the temporal coverage of the Sentinel-1 derived seasonal deformation."*

3. Figure 9c: There is a spelling error in the labels.

Response: Thank you for noting this error. The spelling error in the label of Figure 9c has been corrected in the revised manuscript.

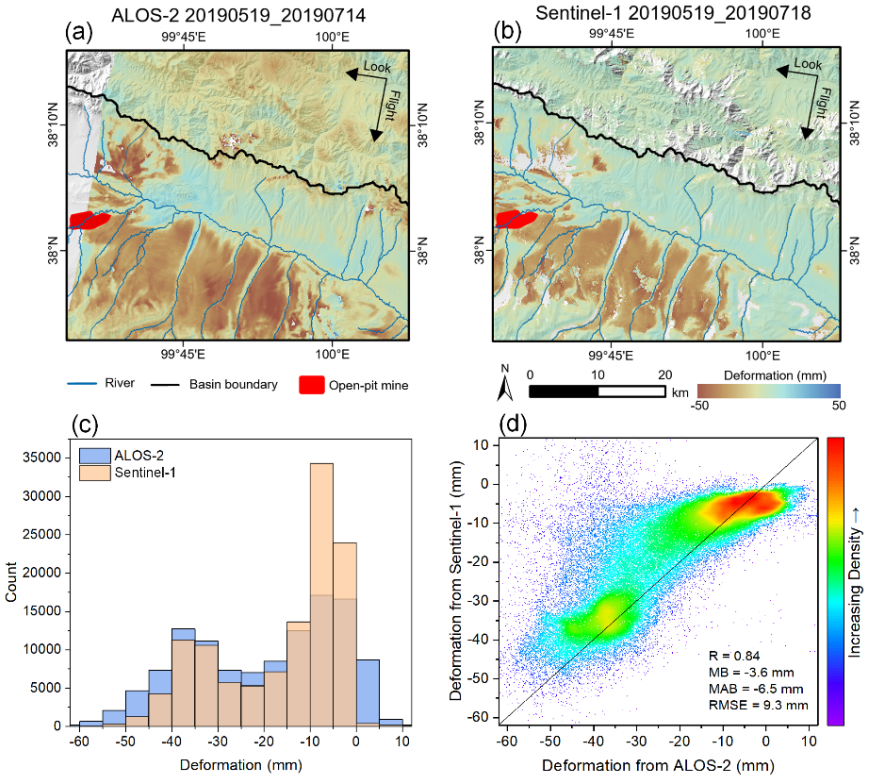

Fig. R7 (Revised Figure 9). Comparison of surface deformation derived from ALOS-2 L-band and Sentinel-1 C-band data during a similar period of the thawing season in 2019: (a) ALOS-2-derived deformation from May 19th to July 14th, 2019; (b) Sentinel-1-derived deformation from May 19th to July 18th, 2019. (c) Histogram distributions of the two deformation maps; (d) Density scatter plot of the two deformation maps with the correlation and difference statistics, including correlation coefficient (R), mean bias (MB), mean absolute bias (MAB), and RMSE.

4. Figure 14: Is the statistical analysis of environmental factors and deformation limited to the study area? How do the authors explain why the northeastern part (outside the study area) shows low albedo values but does not exhibit strong subsidence signals (e.g. as shown in Fig. 13)?

Response: Thank you for raising this point. The statistical analysis between environmental factors and deformation was conducted within the study area boundary, not over the entire map extent shown in Fig. 13. We have clarified the spatial extent of the analysis in the revised manuscript. The low SWIR albedo areas in the northeastern part of the map are mainly distributed along the river valleys underlain by non-permafrost or seasonally frozen ground. Their low albedo likely reflects moist alluvial sediments and river channels rather than thaw of ice-rich permafrost. Some low albedo areas also occur in mountainous permafrost terrain and may reflect surface wetting caused by snowmelt. However, the steep slopes and relatively low ground ice content of these complex mountain areas limit the development of pronounced thaw-related subsidence.

Line 276-: *"……, and all statistical analyses were restricted to pixels within the study area boundary."*